Published in final edited form as:
Biomaterials. 2014 August ; 35(25): 6698–6706. doi:10.1016/j.biomaterials.2014.05.008.

The effect of inflammatory cell-derived MCP-1 loss on neuronal survival during chronic neuroinflammation

Andrew J. Sawyer[1], **Weiming Tian**[2], **Jennifer K. Saucier-Sawyer**[3], **Paul J. Rizk**[4], **W. Mark Saltzman**[3], **Ravi Bellamkonda**[5], and **Themis R. Kyriakides**[1,3]

[1]Departmentof Pathology, Yale School of Medicine, 310 Cedar Street LH 108, New Haven, CT 06520-8023, USA

[2]Bio-X Center, School of Life Science and Technology, Harbin Institute of Technology, Harbin, 150080 P R China

[3]Department of Biomedical Engineering, Yale University, New Haven, CT

[4]Department of Molecular, Cellular and Developmental Biology, Yale University, New Haven, CT

[5]Department of Biomedical Engineering, Georgia Institute of Technology, Atlanta, GA 30332

Abstract

Intracranial implants elicit neurodegeneration via the foreign body response (FBR) that includes BBB leakage, macrophage/microglia accumulation, and reactive astrogliosis, in addition to neuronal degradation that limit their useful lifespan. Previously, monocyte chemoattractant protein 1 (MCP-1, also CCL2), which plays an important role in monocyte recruitment and propagation of inflammation, was shown to be critical for various aspects of the FBR in a tissue-specific manner. However, participation of MCP-1 in the brain FBR has not been evaluated. Here we examined the FBR to intracortical silicon implants in MCP-1 KO mice at 1, 2, and 8 weeks after implantation. MCP-1 KO mice had a diminished FBR compared to WT mice, characterized by reductions in BBB leakage, macrophage/microglia accumulation, and astrogliosis, and an increased neuronal density. Moreover, pharmacological inhibition of MCP-1 in implant-bearing WT mice maintained the increased neuronal density. To elucidate the relative contribution of microglia and macrophages, bone marrow chimeras were generated between MCP-1 KO and WT mice. Increased neuronal density was observed only in MCP-1 knockout mice transplanted with MCP-1 knockout marrow, which indicates that resident cells in the brain are major contributors. We hypothesized that these improvements are the result of a phenotypic switch of the macrophages/microglia polarization state, which we confirmed using PCR for common activation markers. Our observations suggest that MCP-1 influences neuronal loss, which is integral to the progression of

Corresponding authors: Themis Kyriakides, PO Box 208089, New Haven, CT 06509-8089, 203-737-2214, Themis.kyriakides@yale.edu.

neurological disorders like Alzheimer's and Parkinson disease, via BBB leakage and macrophage polarization.

Keywords

Foreign body response; MCP-1; Neurodegeneration; microglia polarization

1. Introduction

Neuronal loss or neurodegeneration occurs as a part of the inflammatory response to both age-related disease and acute injury and can result in either gradual decline of function as seen in Alzheimer's disease, Parkinson's disease, and ALS or the sudden and traumatic loss of function observed in stroke and traumatic brain injury [1, 2]. Intracranial implants elicit a foreign body response (FBR) that involves both short term neuronal damage from the trauma associated with implantation, and prolonged neuroinflammation from the presence of an implant [3]. Therefore, it is a unique model to examine the influence of inflammation on neuronal loss.

Typically, the brain FBR involves the implantation of intracranial stimulating or recording electrodes. The latter are designed to record signals from local neurons and create an interface between the brain and an external computer [4, 5]. This technology is currently used for cochlear implants [4, 6], visual prosthetics [7], motor control [8], and prosthetic limbs [9–11]. However, the FBR, which is distinct from the injury-induced inflammatory response that occurs during the implantation of the electrode, is a barrier to achieving a long implant lifetime [3, 12]. In the brain the FBR involves disruption of the blood-brain barrier (BBB), recruitment and activation of macrophages and local microglia, hypertrophy and hyperproliferation of reactive astrocytes to form the glial scar, and local neurodegeneration [12–15]. Glial scar formation serves as a barrier between the implant and the tissue, decreasing signal strength [16]. FBR-induced BBB disruption, with gaps as large as 500 nm, allows serum proteins to enter into the tissue and contributes to prolonged neuroinflammation [14, 15].

Advances in implant design and drug delivery have been used to ameliorate the FBR and prolong implant life. Decreasing implant stiffness, or method of tethering, can reduce the micromotion caused by the difference in stiffness between the brain and the implant. Decreasing micromotion decreased neuroinflammation and has been shown to decrease the FBR [3, 17–19]. Beyond physical consideration, implant surface and functionality can be altered. Traditional implants are machined from silicon, the use of alternate materials including parylene or bulk metallic glasses can alter the tissue response [20, 21]. One method of altering electrodes is the incorporation of a polyethylene glycol (PEG) coating. PEG coatings bind water to increase the biocompatibility of implants, in the brain these coatings can reduce glial scarring [22]. As an alternative, implants, and implant coatings, have also been used to deliver anti-inflammatory drugs to reduce local neuroinflammation [23–26]. In addition, limiting BBB breach can also improve the FBR [27, 28].

A decrease in the severity of the tissue response during the FBR, as determined histologically via inflammatory cell presence, reactive gliosis, BBB leakage and neuronal loss, results in an improved implant lifetime [29–31]. One possible mechanism is that neuronal loss from the near-implant tissue impairs the recording and signaling capabilities of the electrodes. Factors including the influx of neuronotoxic molecules from the serum due to BBB breach and the production of pro-inflammatory cytokines from local reactive astrocytes, microglia, and macrophages are thought to contribute to neurodegeneration [28]. Moreover, the activation state of, and cytokine production by, macrophages and microglia are key mediators in the propagation of neuroinflammation and neurodegenerative diseases [32, 33]. When microglia are activated they secrete a variety of inflammatory signals, including TNF-α and IL-1β, these and other cytotoxic factors can then induce neuronal death [33].

Upon activation, macrophages and microglia can be induced towards different phenotypes including M1 or classically activated and M2 or alternatively activated [34, 35]. M1 cells are primarily phagocytic and pro-inflammatory whereas M2 cells are associated with tissue repair. M2 cells are divided further into M2a, M2b, M2c, and M2d (tumor associated) based on gene expression profiles and specialized functions. Each activation state induces varying degrees of neuronotoxicity, with M2a inducing the least neurodegeneration [36]. In the brain, the inflammatory response is mediate by both resident microglia and recruited macrophages. In adult mice the relative contributions from these two cell populations can be determined by generating bone marrow chimeras. For example, lethally irradiated WT mice can be rescued with bone marrow from mice that constitutively express green fluorescent protein resulting in monocytes and macrophages that fluoresce green, whereas the resident microglia remain unchanged [37]. This method can be combined with genetic knockout mice to compare the effect of inflammatory defects in either the microglial or macrophage populations [38].

Examining the phenotypic changes in the FBR observed in knockout animal models provides a basis for the rational design of therapeutic interventions. Previously we have used mice that lack either the collagenase matrix metalloproteinase 9 (MMP-9), or the anti-angiogenic matricellular protein thrombospondin 2 (TSP-2), to illustrate the role of the BBB in the FBR [14, 39]. In both cases the leakage of serum protein was increased, which correlated with a more severe FBR. In the current study we examined the role of monocyte chemoattractant protein 1 (MCP-1, also known as CCL-2). MCP-1 is a chemokine whose secretion is induced by inflammatory signals, creating a gradient that attracts monocytes to sites of inflammation. While MCP-1 is expressed by a wide variety of cells, in the CNS microglia and macrophages are the primary sources. More importantly, the response to MCP-1 is regulated by the expression of its receptor, CCR2 [40, 41].

Primary roles of MCP-1 in the CNS include induction of cellular migration, BBB alteration, and inflammation propagation [42]. When MCP-1 is either inhibited or deleted, the compromised monocytes show reduced migration, recruitment, and altered cytokine expression [43, 44]. Commensurate with its role in monocyte transmigration, MCP-1 has been shown to alter BBB permeability by altering tight junction and adherens junction proteins—claudins, cadherins, and zona occludens [45–47]. MCP-1 is also a key mediator in

the inflammatory process, where MCP-1 signaling induces the production of numerous pro-inflammatory cytokines.

In the present study we examined our hypothesis that the absence of MCP-1 would reduce neuroinflammation as a consequence of the FBR via a clinically relevant model implant in MCP-1 knockout mice. A single probe from a Michigan implant was placed in the cortex for up to 8 weeks and the tissue was examined for histological markers of FBR induced neuroinflammation. Additionally, the phenotype of the near-implant macrophages/microglia was examined to identify changes in polarization due to MCP-1 loss. Furthermore, bone marrow chimeric mice were able to identify whether these changes could be attributed to local or circulating inflammatory cells. Finally, pharmacological inhibition of CCR2 for two weeks was used to recapitulate the response of the knockout mouse and show a method of pharmacological intervention that can reduce FBR-induced neuroinflammation, which could increase the lifespan of intracranial implants.

2. Materials and Methods

2.1 Animal models

All animal experiments were performed according to protocols approved by the Yale Institutional Animal Care and Use Committee (IACUC). 12 week old C57Bl6 and MCP-1 KO mice were purchased from Jackson Labs. Model neural implants were implanted into the cortex of anesthetized mice according to a previously described procedure [15, 39]. Briefly, under isofluorane anesthesia their scalps were shaved and subsequently sterilized using alternating alcohol and betadine wipes. A midline incision was made along the scalp and a burr hole was drilled in the skull at 1mm lateral to bregma using a high speed drill. A single shank from a model Michigan-style electrode, made of silicon with a 100 × 15 μm cross-section (NeuroNexus), was inserted through the burr hole and into the brain. The scalp wound was sutured closed and the mouse was removed to a clean cage to recover with free access to food and water. Six mice were used for each genotype at each time point.

After either 1, 2, or 8 weeks the mice were euthanized via transcardial perfusion and fixation with 15 mL of PBS and 15 mL of 4% paraformaldehyde. The brain was removed and further fixed overnight in 4% paraformaldehyde. After fixation the implant was removed and the brain was prepared for histology.

An additional group of C57Bl6 mice were given a CCR2 inhibitor to block MCP-1 activity. Implant-bearing mice (six per group) were given a daily intraperitoneal injection of RS 102895 (Santa Cruz Biotechnology) dissolved in DMSO at a concentration of 3.0 mg/kg or DMSO only. These mice were euthanized at 2 weeks and their brains were prepared for histology as described above.

Bone marrow transplants were used to generate chimeric mice and compare local and circulating sources of MCP-1. BL6 and MCP-1 KO mice were given a lethal dose of 10Gy using an x-ray irradiator (Marietta model PXR 014). After irradiation, the animals were given a tail vein injection of 1×10^6 donor bone marrow cells isolated from the femurs of either Bl6 or MCP-1 KO mice. Chimeric and syngeneic transplants were completed,

resulting in four groups: WT^{WT}, WT^{KO}, KO^{WT}, and KO^{KO}, named so uppercase letter is the background and the superscript letter indicate the bone marrow genotype. These animals received brain implants 4 weeks after rescue. The implants were removed and the tissue was analyzed 2 weeks after implantation. Four mice each were used for WT^{WT}, WT^{KO}, and KO^{WT} groups, six mice were used for KO^{KO} group.

2.2 QPCR Analysis

Six C57Bl6 and six MCP-1 KO mice were given intracranial implants as described above. After two weeks the brain was removed and the tissue surrounding the implant was isolated using a 2mm biopsy punch. The tissue sample was immediately immersed in RNAlater (Qiagen). RNA was extracted using an RNeasy Lipid tissue mini kit (Qiagen). 1 ug of RNA was transcribed using the Quantitect reverse transcription kit (Qiagen). Levels of gene expression were determined using SYBR green supermix and the CFX96 Real time PCR from Bio-Rad. Gene expression was normalized to GAPDH. Mouse-specific forward and reverse primer sequences are: CD 68 (5′-TGTCTGATCTTGCTAGGACCG-3′ and 5′-GAGAGTAACGGCCTTTTTGTGA-3′), CCR7 (5′-TGTACGAGTCGGTGTGCTTC-3′ and 5′-GGTAGGTATCCGTCATGGTCTTG-3′), CD 80 (5′-GCAGGATACACCACTCCTCAA-3′ and 5′-AAAGACGAATCAGCAGCACAA-3′), CD 163 (5′-CTGGCCTCTGAGTTTAGGGTC-3′ and 5′-CCCTTGGTGTCGAACCAGC-3′), CD 206 (5′-GGCAGGATCTGGCAACCTAGTA-3′ and 5′-GTTTGGATCGGCACACAAAGTC-3′), and Arg1 (5′-TTGGGTGGATGCTCACACTG-3′ and 5′-TTGCCCATGCAGATTCCC-3′).

2.3 Histology

Transverse paraffin sections of fixed brain tissue were prepared by the Yale Research Histology service. H&E stain was used to observe general histology. Immunohistochemical stains were completed using antibodies against NeuN, GFAP, Mac-3, and mouse serum albumin (MSA) at dilutions of 1:100, 1:2500, 1:50, and 1:1000 respectively. Tissues stained for MSA were visualized using an Alexa 488 conjugated secondary antibody (Life Technologies), mounted using Vectashield with DAPI (Vector Labs), and imaged using a Zeiss Axiovert 200M fluorescent microscope with Volocity software (Perkin Elmer). All other antibodies were incubated with appropriate biotinylated secondary antibodies, and stained using the ABC peroxidase standard and DAB kits from Vector Labs. Endogenous peroxidase activity was blocked with a solution of 3% hydrogen peroxide and 0.1% sodium azide in methanol. Nonspecific binding was blocked using 1% BSA for all antibodies. Peroxidase stained tissues were imaged using a Axioimager A1 microscope and Axiocam mHRC camera with Axiovision software (Carl Zeiss). The amount of stain in each field was quantified using Metamorph software (Molecular Devices). Statistical analysis was conducted using Prizm (GraphPad).

3. Results

3.1 Reduced neuroinflammation and neurodegeneration in MCP-1 KO mice

Model silicon implants were used in this study to induce a typical FBR in the cortex. Silicon implant arrays are used extensively both clinically and in brain-computer interface research

[10, 29]. Tissue sections from implant bearing mice were stained with H&E to reveal general tissue histology. MCP-1 KO mice showed reduced signs of inflammation at 1, 2, and 8 weeks after implantation (Figure 1). WT mice showed signs of matrix degradation and vacuoles in the tissue. Hemosiderin laden macrophages were also clearly visible, the intense brown color caused by the breakdown of erythrocytes that indicate local hemorrhage (Figure 1H).

Degenerating neurons were visible in the vicinity of the implants in WT tissue sections. These neurons show pyknotic nuclei and eosinophillic cytoplasm, and were located near the implant cavity [48]. Their physical characteristics, location, and lack of corkscrew dendrites distinguish them from the “dark neurons” that are a common histological artifact [49]. In contrast, sections of MCP-1 KO mice contained abundant healthy neurons at 8 weeks.

Sections were stained for NeuN to show neuronal nuclei near the implant (Figure 2). At 1 week, when the FBR was likely dominated by the trauma from implant insertion, there was no difference in neuronal density between WT and MCP1-KO mice. However, an increased amount of neurons in the near implant tissue was observed in MCP1-KO mice, when compared to WT mice, at both 2 and 8 weeks. These neurons appeared healthy under histological examination, and in many cases were within 25 μm of the implant surface. Successive elliptical areas were defined around the implant cavity to determine the neuronal density at specified distances from the implant surface. While there was no difference between KO and WT within 25 μm of the implant, after that distance the neuron positive area was increased in the KO mice (Figure 2J, K).

3.2 Reduced Inflammation in MCP-1 KO mice

Immunohistochemical staining was conducted to assess the traditional markers of the FBR. Reactive astrocytes increased in size and number to form a glial scar around the implant as part of the foreign body response (Figure 2). GFAP staining revealed the glial scar, which was visible along the implant cavity at all time points. Intense staining also appeared around near-implant blood vessels, highlighting the role of astrocytes in maintaining the BBB. Reactive gliosis was most pronounced at 1 and 2 weeks after implantation, and was decreased at eight weeks in the MCP-1 KO mice (Figure 2B, F, and L).

BBB compromise has been recognized as a complication to the brain FBR [14, 39, 50]. Immunohistochemical staining for mouse serum albumin, which is excluded by an intact BBB, was conducted to indicate the presence of BBB compromise (Figure 2C, G, M). BBB leakage was greatest initially after implantation and resolved over time. After eight weeks MCP-1 KO mice showed significantly less leakage than WT, indicating a better functioning BBB. When taken together with the decrease in astrogliosis and the improved neuronal density, these factors indicate reduced neuroinflammation in the MCP-1 KO mice.

3.3 Macrophage/microglia response

The presence of macrophages/microglia was generally reduced in the MCP-1 KO mice, with the exception of the 2 week timepoint where there was a significant increase in inflammatory cells (Figure 2D, H, N). Macrophages and microglia are an important part of both the propagation and resolution of neuroinflammation; however, increased inflammatory

cell presence is generally indicative of increased inflammation. In this case, MCP-1 KO macrophages/microglia may exhibit phenotypic differences that alter their behavior as part of the FBR. Therefore, in addition quantification of macrophages/microglia, we used quantitative real-time PCR to measure the levels of M1 (CCR7, CD 80) and M2 (CD 163, CD 206, and Arg-1) activation markers (Figure 3). M1 markers were either unchanged (CCR7) or increased (CD80) when comparing MCP-1 KO to WT samples. In contrast, all M2 markers (CD 163, CD 206, and Arg-1) were increased in MCP-1 KO mice. While the tissue sample contained a diverse population of cells, the markers we analyzed are all primarily expressed on cells of monocyte/macrophage lineage. Therefore, we speculate that the increased levels of M2-associated markers indicate a phenotypic shift in the MCP-1 KO macrophages towards a decreased inflammatory state.

3.4 Inhibition of CCR2

In order to recapitulate the FBR of the MCP-1 KO mice, implant-bearing animals were given a daily IP injection of RS 102895 for two weeks. RS 102895 is a CCR2 antagonist that blocks the activity of MCP-1 [51, 52]. A dose of either 3.0 mg/kg RS 102895 or DMSO (vehicle) was given to separate cohorts of six mice to inhibit the function of CCR2. The dose was selected based on its efficacy in previously published studies [53, 54].

Mice that received the vehicle injections elicited a FBR similar to that of WT mice. Specifically, BBB leakage, macrophage/microglia accumulation and reactive astrogliosis were similar between WT and vehicle-injected mice. However, there was a decrease in neuronal density in vehicle-injected mice, which could indicate some degree of DMSO toxicity.

Similar to the MCP-1 KO mice, pharmacological inhibition of CCR2 yielded a significant increase neuronal density in the peri-implant tissue (Figure 4C). Additional markers of inflammation were also improved with CCR2 inhibition including reactive astrogliosis, BBB leakage, and inflammatory cell accumulation (Figure 4D, E, and F). Taken together, these observations suggest that administration of the CCR2 inhibitor reduced neuroinflammation.

3.5 Bone marrow MCP-1 chimeras

In order to determine whether MCP-1 in the FBR is produced by resident or recruited cells, bone marrow chimeras were generated using MCP-1 KO and WT mice. Lethally irradiated recipients were rescued with bone marrow from either KO or WT mice. Four weeks after transplantation each mouse received one intracortical implant. Two weeks later the animals were euthanized and the brain tissue was prepared for histology.

Analysis of NeuN deposition by immunohistochemistry showed that KO^{KO} mice (MCP-1 KO mice rescued with MCP-1 KO bone marrow) maintained an increased neuronal density when compared to WT^{WT} mice (Bl6 mice rescued with Bl6 bone marrow) (Figure 5). Rescuing BL6 mice with KO bone marrow (WT^{KO}) restricted MCP-1 expression to resident cells, and resulted in a small increase in neuronal density. A similar increase in neuronal density was observed in KO^{WT} mice, where the major source of MCP-1 is from circulating cells. The inflammatory cell increase observed in the KO mouse was also observed in the KO^{KO} group, which also saw a small decrease in reactive astrogliosis. BBB leakage also

appeared to decrease in both KO^{WT} and KO^{KO} mice, suggesting that the response is dominated by the host cells.

4. Discussion

In the present study we examined the role of MCP-1 in the brain FBR. In order to induce the FBR, a single shank from an electrode made of clinically relevant material was used to elicit BBB leakage, activation and recruitment of macrophages/microglia, reactive astrogliosis, and neuronal degeneration: traditional aspects of the FBR that we quantified. Analysis showed that there was no difference between MCP-1 KO and WT mice at 1 week, at a time when the FBR is dominated by the acute trauma of implantation. However, during the chronic phase of the FBR, measured at 8 weeks, MCP-1 KO mice showed an improved tissue reaction, evidenced by reduced astrogliosis, decreased inflammatory cell presence, improved BBB function, and greater neuronal density.

MCP-1 is a primary inflammatory messenger and chemoattractant. For example, when brain cells are exposed to serum albumin, possibly due to BBB compromise, MCP-1 production is rapidly upregulated [55]. MCP-1 signaling is also increased when there is neuronal damage and astrogliosis independent of BBB compromise [56]. In neurodegenerative disease, MCP-1 is a reliable marker and a key mediator for chronic neuroinflammation observed in Alzheimer's disease, Huntington's disease, ALS, and MS [57]. In addition, MCP-1 signaling is involved in brain injury and the FBR in the body, making it a likely mediator in the brain FBR [58–60].

Decreased neurodegeneration in MCP-1 KO mice was striking. Specifically, abundant healthy neurons were observed in close proximity to the implant cavity at both 2 and 8 weeks. Increased neuronal density is important because maintaining healthy neurons near the electrode is critical for preserving implant performance [61]. In attempting to decrease neurodegeneration, earlier research has focused on delivery of neurotrophic factors, steroids, or implant coatings to induce neuron ingrowth [61–63]. As presented here, phenotypic changes induced by genetic knockout of MCP-1 can provide improvements in neuronal density, while decreasing additional markers of neuroinflammation and the FBR, suggesting an alternate avenue for neuroprotective therapies.

Because MCP-1 expression is associated with macrophage activation, we asked whether the improved FBR in MCP-1 KO mice was due to a dysfunction in the macrophages and local microglia. Therefore, we determined the expression of common macrophage/microglia activation markers in the FBR of WT and MCP-1 KO mice. Our results indicated that the macrophages/microglia were skewed towards an alternatively activated repair and regeneration phenotype at 2 weeks. Previous research has shown that this phenotype is associated with decreased neuronal loss, which may account for the decreased neurodegeneration observed in the MCP-1 KO mice [36]. Biasing the phenotype of the macrophages/microglia presents an attractive therapeutic strategy, which can alter tissue responses without necessarily influencing the number of local inflammatory cells [64–66].

We have also shown that the pharmacological inhibition of MCP-1 also ameliorates the FBR. The drug RS 1028985 is known antagonist of CCR2, with the ability to block MCP-1

binding and reduce the migration of macrophages [52]. When implant-bearing WT mice were given a daily IP dose of RS 102895 they showed increased neuronal density, reduced astrogliosis, improved BBB function, and reduced inflammatory cell presence when compared to mice administered the vehicle. Our observations suggest that the improved FBR observed in the MCP-1 KO mouse can be duplicated therapeutically in WT mice.

It should be noted that there are some important distinctions between genetic knockouts and the pharmacological inhibition presented in this study. In global KO models, additional pathways can be engaged as adoptive responses to the loss of a single gene. The effect of MCP-1 deletion proceeds in a tissue specific manner. For example, when MCP-1 KO mice receive an intraperitoneal injection of thioglycolate, which causes inflammation, they show decreased macrophage accumulation when compared to WT mice [43]. In contrast, macrophage recruitment was not reduced in MCP-1 KO mice in skin wound, subcutaneous implant, and intraperitoneal implant models [59, 60, 67]. In this study we observed an increased macrophage/microglia accumulation at two weeks in both MCP-1 KO and KO^{KO} mice. A compensatory mechanism, or alterations in BBB permeability affecting monocyte migration, could explain the increased inflammatory cell presence.

In contrast to the MCP-1 KO and KO^{KO} mice, the administration of the CCR2 antagonist significantly decreased inflammatory cell presence at 2 weeks. However, the increase in neuronal density persisted. Without increasing the total amount of inflammatory cells, pharmacological inhibition could alter the amount of macrophages present in the CNS relative to the amount of microglia. Macrophages and microglia respond in different ways to identical stimuli, and alterations to the macrophage/microglia ratio could alter the outcome of the FBR [68].

5. Conclusions

We have shown that both genetic knockout and pharmacological inhibition of MCP-1 improve the FBR in the brain. A primary benefit in both models is the preservation of neurons near the implant that are critical for implant function. These results indicate that inhibition of MCP-1 could be a promising therapy for improving the lifetime of chronically implanted neural electrodes.

Acknowledgments

The authors would like to acknowledge Dr. Jung Kim, Dr. Joe Madri, and Dr. Anita Huttner for their assistance in examining brain tissue sections. This research was funded by NIH grant RO1GM072194, NIH vascular research training grant T32HL007950, and by the Defense Advanced Research Projects Agency (DARPA) MTO under the auspices of Dr. Jack Judy through the Space and Naval Warfare Systems Center, Pacific Grant/Contract No. N66001-11-1-RB420-G1.

References

1. Glass CK, Saijo K, Winner B, Marchetto MC, Gage FH. Mechanisms underlying inflammation in neurodegeneration. Cell. 2010; 140:918–34. [PubMed: 20303880]
2. Allan SM, Tyrrell PJ, Rothwell NJ. Interleukin-1 and neuronal injury. Nat Rev Immunol. 2005; 5:629–40. [PubMed: 16034365]

3. Polikov VS, Tresco PA, Reichert WM. Response of brain tissue to chronically implanted neural electrodes. J Neurosci Methods. 2005; 148:1–18. [PubMed: 16198003]
4. Nicolelis MA. Actions from thoughts. Nature. 2001; 409:403–7. [PubMed: 11201755]
5. Friehs GM, Zerris VA, Ojakangas CL, Fellows MR, Donoghue JP. Brain-machine and brain-computer interfaces. Stroke. 2004; 35:2702–5. [PubMed: 15486335]
6. Wilson BS, Finley CC, Lawson DT, Wolford RD, Eddington DK, Rabinowitz WM. Better speech recognition with cochlear implants. Nature. 1991; 352:236–8. [PubMed: 1857418]
7. Hetling JR, Baig-Silva MS. Neural prostheses for vision: designing a functional interface with retinal neurons. Neurol Res. 2004; 26:21–34. [PubMed: 14977054]
8. Dhillon GS, Horch KW. Direct neural sensory feedback and control of a prosthetic arm. IEEE Trans Neural Syst Rehabil Eng. 2005; 13:468–72. [PubMed: 16425828]
9. Donoghue JP. Connecting cortex to machines: recent advances in brain interfaces. Nat Neurosci. 2002; 5 (Suppl):1085–8. [PubMed: 12403992]
10. Hochberg LR, Bacher D, Jarosiewicz B, Masse NY, Simeral JD, Vogel J, et al. Reach and grasp by people with tetraplegia using a neurally controlled robotic arm. Nature. 2012; 485:372–5. [PubMed: 22596161]
11. Donoghue JP, Nurmikko A, Black M, Hochberg LR. Assistive technology and robotic control using motor cortex ensemble-based neural interface systems in humans with tetraplegia. Physiol J. 2007; 579:603–11.
12. McConnell GC, Rees HD, Levey AI, Gutekunst CA, Gross RE, Bellamkonda RV. Implanted neural electrodes cause chronic, local inflammation that is correlated with local neurodegeneration. J Neural Eng. 2009; 6:056003. [PubMed: 19700815]
13. Biran R, Martin DC, Tresco PA. Neuronal cell loss accompanies the brain tissue response to chronically implanted silicon microelectrode arrays. Exp Neurol. 2005; 195:115–26. [PubMed: 16045910]
14. Tian W, Kyriakides TR. Matrix metalloproteinase-9 deficiency leads to prolonged foreign body response in the brain associated with increased IL-1beta levels and leakage of the blood-brain barrier. Matrix Biol. 2009; 28:148–59. [PubMed: 19264129]
15. Sawyer AJ, Kyriakides TR. Nanoparticle-based evaluation of blood-brain barrier leakage during the foreign body response. J Neural Eng. 2013; 10:016013. [PubMed: 23337399]
16. McConnell GC, Butera RJ, Bellamkonda RV. Bioimpedance modeling to monitor astrocytic response to chronically implanted electrodes. J Neural Eng. 2009; 6:055005. [PubMed: 19721187]
17. Thelin J, Jorntell H, Psouni E, Garwicz M, Schouenborg J, Danielsen N, et al. Implant size and fixation mode strongly influence tissue reactions in the CNS. PLoS One. 2011; 6:e16267. [PubMed: 21298109]
18. Biran R, Martin DC, Tresco PA. The brain tissue response to implanted silicon microelectrode arrays is increased when the device is tethered to the skull. J Biomed Mater Res A. 2007; 82:169–78. [PubMed: 17266019]
19. Rousche PJ, Pellinen DS, Pivin DP Jr, Williams JC, Vetter RJ, Kipke DR. Flexible polyimide-based intracortical electrode arrays with bioactive capability. IEEE Trans Biomed Eng. 2001; 48:361–71. [PubMed: 11327505]
20. Seymour JP, Kipke DR. Neural probe design for reduced tissue encapsulation in CNS. Biomaterials. 2007; 28:3594–607. [PubMed: 17517431]
21. Schroers J, Kumar G, Hodges TM, Chan S, Kyriakides TR. Bulk Metallic Glasses for Biomedical Applications. JOM. 2009; 61:8.
22. Rao L, Zhou H, Li T, Li C, Duan YY. Polyethylene glycol-containing polyurethane hydrogel coatings for improving the biocompatibility of neural electrodes. Acta Biomater. 2012; 8:2233–42. [PubMed: 22406507]
23. He W, McConnell GC, Bellamkonda RV. Nanoscale laminin coating modulates cortical scarring response around implanted silicon microelectrode arrays. J Neural Eng. 2006; 3:316–26. [PubMed: 17124336]
24. He W, McConnell GC, Schneider TM, Bellamkonda RV. A novel anti-inflammatory surface for neural electrodes. Adv Mater. 2007; 19:3529.

25. Zhong YH, Bellamkonda RV. Controlled release of anti-inflammatory agent alpha-MSH from neural implants. J Control Release. 2005; 106:309–18. [PubMed: 15978692]
26. Zhong YH, Bellamkonda RV. Dexamethasone-coated neural probes elicit attenuated inflammatory response and neuronal loss compared to uncoated neural probes. Brain Res. 2007; 1148:15–27. [PubMed: 17376408]
27. Kozai TD, Marzullo TC, Hooi F, Langhals NB, Majewska AK, Brown EB, et al. Reduction of neurovascular damage resulting from microelectrode insertion into the cerebral cortex using in vivo two-photon mapping. J Neural Eng. 2010; 7:046011. [PubMed: 20644246]
28. Saxena T, Karumbaiah L, Gaupp EA, Patkar R, Patil K, Betancur M, et al. The impact of chronic blood-brain barrier breach on intracortical electrode function. Biomaterials. 2013; 34:4703–13. [PubMed: 23562053]
29. Karumbaiah L, Saxena T, Carlson D, Patil K, Patkar R, Gaupp EA, et al. Relationship between intracortical electrode design and chronic recording function. Biomaterials. 2013; 34:8061–74. [PubMed: 23891081]
30. Karumbaiah L, Norman SE, Rajan NB, Anand S, Saxena T, Betancur M, et al. The upregulation of specific interleukin (IL) receptor antagonists and paradoxical enhancement of neuronal apoptosis due to electrode induced strain and brain micromotion. Biomaterials. 2012; 33:5983–96. [PubMed: 22681976]
31. Prasad A, Xue QS, Sankar V, Nishida T, Shaw G, Streit WJ, et al. Comprehensive characterization and failure modes of tungsten microwire arrays in chronic neural implants. J Neural Eng. 2012; 9:056015. [PubMed: 23010756]
32. Dheen ST, Kaur C, Ling EA. Microglial activation and its implications in the brain diseases. Curr Med Chem. 2007; 14:1189–97. [PubMed: 17504139]
33. Smith JA, Das A, Ray SK, Banik NL. Role of pro-inflammatory cytokines released from microglia in neurodegenerative diseases. Brain Res Bull. 2012; 87:10–20. [PubMed: 22024597]
34. Gordon S. Alternative activation of macrophages. Nat Rev Immunol. 2003; 3:23–35. [PubMed: 12511873]
35. Boche D, Perry VH, Nicoll JA. Review: activation patterns of microglia and their identification in the human brain. Neuropathol Appl Neurobiol. 2013; 39:3–18. [PubMed: 23252647]
36. Chhor V, Le Charpentier T, Lebon S, Ore MV, Celador IL, Josserand J, et al. Characterization of phenotype markers and neuronotoxic potential of polarised primary microglia in vitro. Brain Behav Immun. 2013; 32:70–85. [PubMed: 23454862]
37. Tanaka R, Komine-Kobayashi M, Mochizuki H, Yamada M, Furuya T, Migita M, et al. Migration of enhanced green fluorescent protein expressing bone marrow-derived microglia/macrophage into the mouse brain following permanent focal ischemia. Neuroscience. 2003; 117:531–9. [PubMed: 12617960]
38. Schilling M, Strecker JK, Schabitz WR, Ringelstein EB, Kiefer R. Effects of monocyte chemoattractant protein 1 on blood-borne cell recruitment after transient focal cerebral ischemia in mice. Neuroscience. 2009; 161:806–12. [PubMed: 19374937]
39. Tian W, Sawyer A, Kocaoglu FB, Kyriakides TR. Astrocyte-derived thrombospondin-2 is critical for the repair of the blood-brain barrier. Am J Pathol. 2011; 179:860–8. [PubMed: 21704005]
40. Deshmane SL, Kremlev S, Amini S, Sawaya BE. Monocyte chemoattractant protein-1 (MCP-1): an overview. J Interferon Cytokine Res. 2009; 29:313–26. [PubMed: 19441883]
41. Yang G, Meng Y, Li W, Yong Y, Fan Z, Ding H, et al. Neuronal MCP-1 mediates microglia recruitment and neurodegeneration induced by the mild impairment of oxidative metabolism. Brain Pathol. 2011; 21:279–97. [PubMed: 21029241]
42. Semple BD, Kossmann T, Morganti-Kossmann MC. Role of chemokines in CNS health and pathology: a focus on the CCL2/CCR2 and CXCL8/CXCR2 networks. J Cereb Blood Flow Metab. 2010; 30:459–73. [PubMed: 19904283]
43. Lu B, Rutledge BJ, Gu L, Fiorillo J, Lukacs NW, Kunkel SL, et al. Abnormalities in monocyte recruitment and cytokine expression in monocyte chemoattractant protein 1-deficient mice. J Exp Med. 1998; 187:601–8. [PubMed: 9463410]
44. Zhang Y, Rollins BJ. A dominant negative inhibitor indicates that monocyte chemoattractant protein 1 functions as a dimer. Mol Cell Biol. 1995; 15:4851–5. [PubMed: 7651403]

45. Stamatovic SM, Shakui P, Keep RF, Moore BB, Kunkel SL, Van Rooijen N, et al. Monocyte chemoattractant protein-1 regulation of blood-brain barrier permeability. J Cereb Blood Flow Metab. 2005; 25:593–606. [PubMed: 15689955]
46. Roberts TK, Eugenin EA, Lopez L, Romero IA, Weksler BB, Couraud PO, et al. CCL2 disrupts the adherens junction: implications for neuroinflammation. Lab Invest. 2012; 92:1213–33. [PubMed: 22641100]
47. Stamatovic SM, Keep RF, Kunkel SL, Andjelkovic AV. Potential role of MCP-1 in endothelial cell tight junction 'opening': signaling via Rho and Rho kinase. J Cell Sci. 2003; 116:4615–28. [PubMed: 14576355]
48. Garman RH. Histology of the central nervous system. Toxicol Pathol. 2011; 39:22–35. [PubMed: 21119051]
49. Jortner BS. The return of the dark neuron. A histological artifact complicating contemporary neurotoxicologic evaluation. Neurotoxicology. 2006; 27:628–34. [PubMed: 16650476]
50. Winslow BD, Tresco PA. Quantitative analysis of the tissue response to chronically implanted microwire electrodes in rat cortex. Biomaterials. 2010; 31:1558–67. [PubMed: 19963267]
51. Mirzadegan T, Diehl F, Ebi B, Bhakta S, Polsky I, McCarley D, et al. Identification of the binding site for a novel class of CCR2b chemokine receptor antagonists: binding to a common chemokine receptor motif within the helical bundle. J Biol Chem. 2000; 275:25562–71. [PubMed: 10770925]
52. Mines M, Ding Y, Fan GH. The many roles of chemokine receptors in neurodegenerative disorders: emerging new therapeutical strategies. Curr Med Chem. 2007; 14:2456–70. [PubMed: 17979699]
53. Rehni AK, Singh N. Ammonium pyrrolidine dithiocarbamate and RS 102895 attenuate opioid withdrawal in vivo and in vitro. Psychopharmacology (Berl). 2012; 220:427–38. [PubMed: 21931991]
54. Rehni AK, Singh TG. Involvement of CCR-2 chemokine receptor activation in ischemic preconditioning and postconditioning of brain in mice. Cytokine. 2012; 60:83–9. [PubMed: 22704692]
55. Calvo CF, Amigou E, Tence M, Yoshimura T, Glowinski J. Albumin stimulates monocyte chemotactic protein-1 expression in rat embryonic mixed brain cells. J Neurosci Res. 2005; 80:707–14. [PubMed: 15880558]
56. Little AR, Benkovic SA, Miller DB, O'Callaghan JP. Chemically induced neuronal damage and gliosis: enhanced expression of the proinflammatory chemokine, monocyte chemoattractant protein (MCP)-1, without a corresponding increase in proinflammatory cytokines(1). Neuroscience. 2002; 115:307–20. [PubMed: 12401343]
57. Bose S, Cho J. Role of chemokine CCL2 and it receptor CCR2 in neurodegenerative diseases. Arch Pharm Res. 2013
58. Grzybicki D, Moore SA, Schelper R, Glabinski AR, Ransohoff RM, Murphy S. Expression of monocyte chemoattractant protein (MCP-1) and nitric oxide synthase-2 following cerebral trauma. Acta Neuropathol. 1998; 95:98–103. [PubMed: 9452827]
59. Skokos EA, Charokopos A, Khan K, Wanjala J, Kyriakides TR. Lack of TNF-alpha-induced MMP-9 production and abnormal E-cadherin redistribution associated with compromised fusion in MCP-1-null macrophages. Am J Pathol. 2011; 178:2311–21. [PubMed: 21514443]
60. Kyriakides TR, Foster MJ, Keeney GE, Tsai A, Giachelli CM, Clark-Lewis I, et al. The CC chemokine ligand, CCL2/MCP1, participates in macrophage fusion and foreign body giant cell formation. Am J Pathol. 2004; 165:2157–66. [PubMed: 15579457]
61. Schwartz AB, Cui XT, Weber DJ, Moran DW. Brain-controlled interfaces: movement restoration with neural prosthetics. Neuron. 2006; 52:205–20. [PubMed: 17015237]
62. He W, Bellamkonda RV. Nanoscale neuro-integrative coatings for neural implants. Biomaterials. 2005; 26:2983–90. [PubMed: 15603793]
63. Shain W, Spataro L, Dilgen J, Haverstick K, Retterer S, Isaacson M, et al. Controlling cellular reactive responses around neural prosthetic devices using peripheral and local intervention strategies. IEEE Trans Neural Syst Rehabil Eng. 2003; 11:186–8. [PubMed: 12899270]
64. Mikita J, Dubourdieu-Cassagno N, Deloire MS, Vekris A, Biran M, Raffard G, et al. Altered M1/M2 activation patterns of monocytes in severe relapsing experimental rat model of multiple

sclerosis. Amelioration of clinical status by M2 activated monocyte administration. Mult Scler. 2011; 17:2–15. [PubMed: 20813772]

65. Mokarram N, Merchant A, Mukhatyar V, Patel G, Bellamkonda RV. Effect of modulating macrophage phenotype on peripheral nerve repair. Biomaterials. 2012; 33:8793–801. [PubMed: 22979988]
66. Zhang L, Cao Z, Bai T, Carr L, Ella-Menye JR, Irvin C, et al. Zwitterionic hydrogels implanted in mice resist the foreign-body reaction. Nat Biotechnol. 2013; 31:553–6. [PubMed: 23666011]
67. Low QE, Drugea IA, Duffner LA, Quinn DG, Cook DN, Rollins BJ, et al. Wound healing in MIP-1alpha(−/−) and MCP-1(−/−) mice. Am J Pathol. 2001; 159:457–63. [PubMed: 11485904]
68. Durafourt BA, Moore CS, Zammit DA, Johnson TA, Zaguia F, Guiot MC, et al. Comparison of polarization properties of human adult microglia and blood-derived macrophages. Glia. 2012; 60:717–27. [PubMed: 22290798]

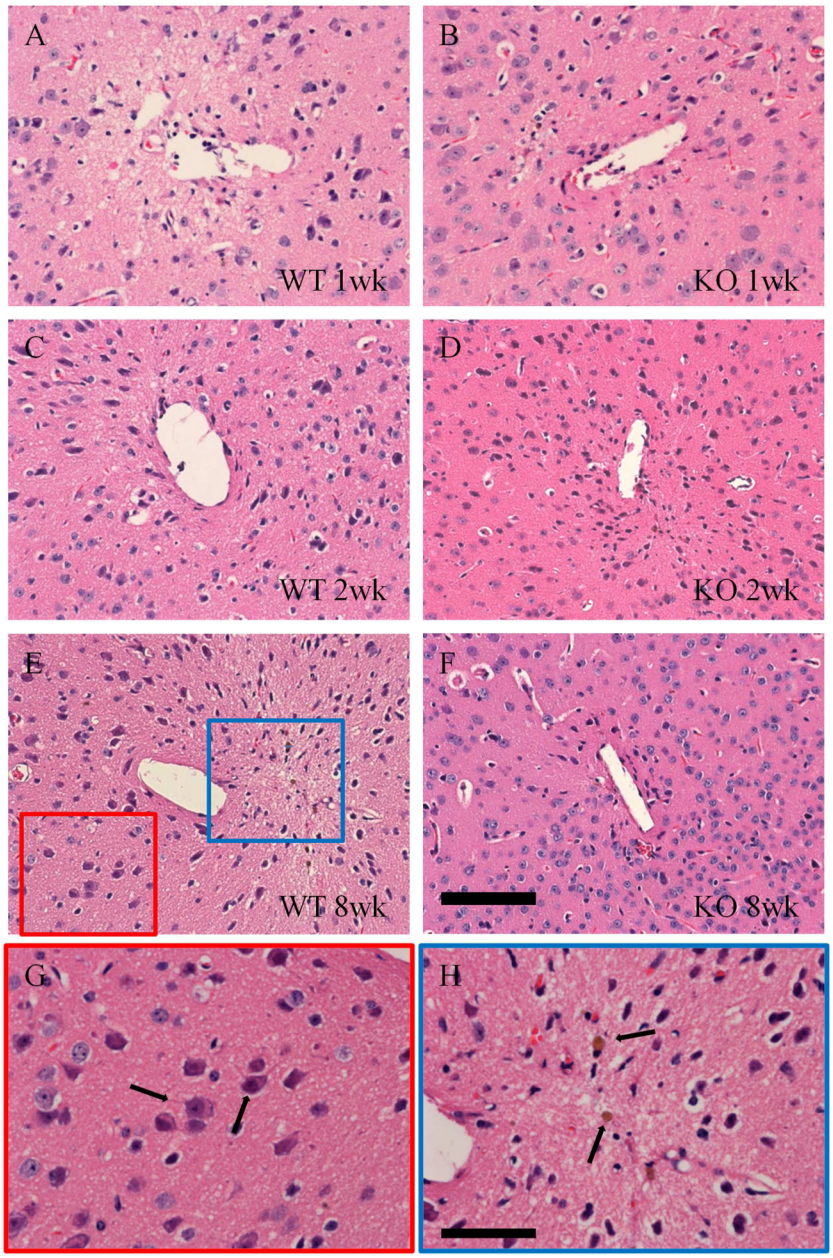

Figure 1.

Neuroinflammation was reduced in MCP-1 KO mice. WT (A, C, E) and MCP-1 KO (B, D, F) tissue were stained with hematoxylin and eosin to reveal overall tissue health. WT tissue showed signs of increased inflammation when compared to KO tissue at all time points, including anoxic degrading neurons (indicated by arrows in G), and hemosiderin laden macrophages (indicated by arrows in H) that indicate tissue hemorrhage. Healthy neurons were increased in KO tissue, particularly at 8 wks (F). Scale is 100 μm in F and 50 μm in H.

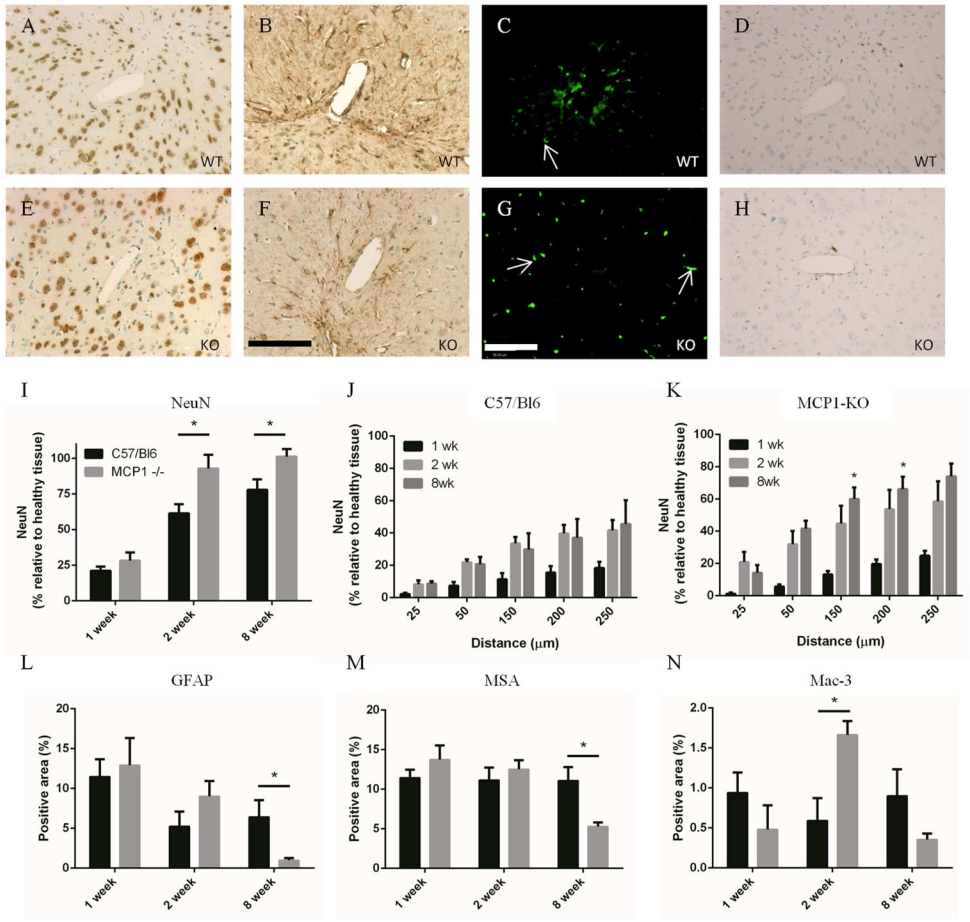

Figure 2.

Neuroinflammation was reduced in MCP-1 KO mice. Paraffin embedded brain sections were stained for NeuN to reveal near-implant neurons. MCP-1 KO (E) tissue showed an increased density of neurons when compared to WT (A) tissue. Quantification of NeuN positive area (I) showed that there was a statistically significant increase in neuronal density at 2 and 8 wks in the KO mice. Elliptical regions were used to quantify the amount of positive stain at distances from the implant interface in WT (J) and KO mice (K). Neuronal density was increased in the KO mice at all distances from the implant cavity (* in K compare WT and KO at the same time and distance). Reactive astrocytes were visible around the wound cavity 1, 2, and 8 wks in both WT (B) and KO (F) mice. The extent of reactive gliosis was reduced in KO mice at 8 wks (L), when quantified using MetaMorph. The presence of MSA was used to measure the extent of BBB leakage. Bright, punctuate areas of fluorescence, visible in all sections but highlighted by white arrows in C, and G, indicate unperfused vessels and were excluded from analysis. Both WT (C) and KO (G) tissue showed extensive leakage at 1 wk which gradually resolved over time (M). At 8 wks, the amount of BBB leakage in KO tissue was less than in WT tissue, which indicates greater BBB integrity and an improved FBR. Tissue sections were stained with Mac-3 to show local macrophage/microglia accumulation. WT mice showed consistent macrophage/microglia presence in WT mice from 1 to 8 wks (D, H, N). Macrophage accumulation peaked at 2 wks

after implantation in the KO mice. Scale is 100 μm in F and G, * indicates $p < 0.05$ using Student's t test, n is 6 for each point and data is presented ± SEM.

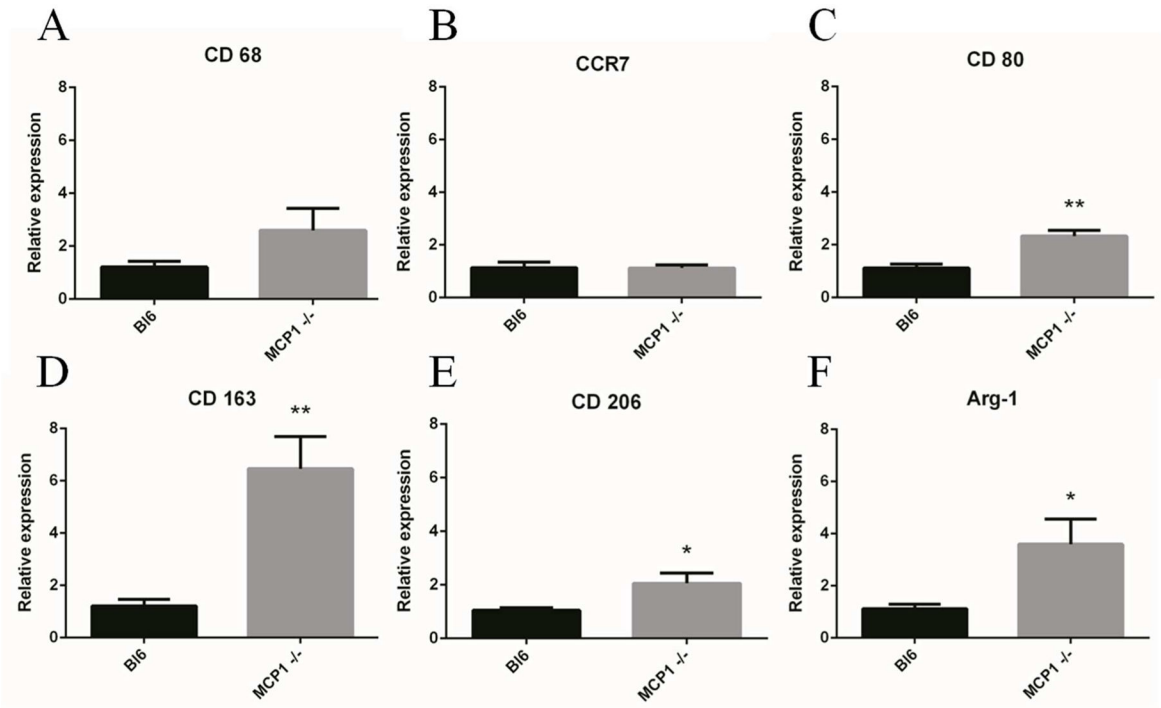

Figure 3.

KO macrophages were shifted towards an M2 phenotype at 2 wks. Quantitative real-time PCR was used to measure markers for macrophage polarization. WT and KO macrophages showed similar levels of CD 68 (A, pan macrophage) and CCR7 (B, M1). The M1 marker CD 80 (C) was elevated in KO mice. The M2 markers CD 163 (D), CD 206 (E), and Arg-1(F) were all elevated in KO mice, which indicated a phenotype shift at two weeks. * indicates $p < 0.05$ and ** indicates $p < 0.01$ using Student's t test, n is 6 for each point and data is presented ± SEM.

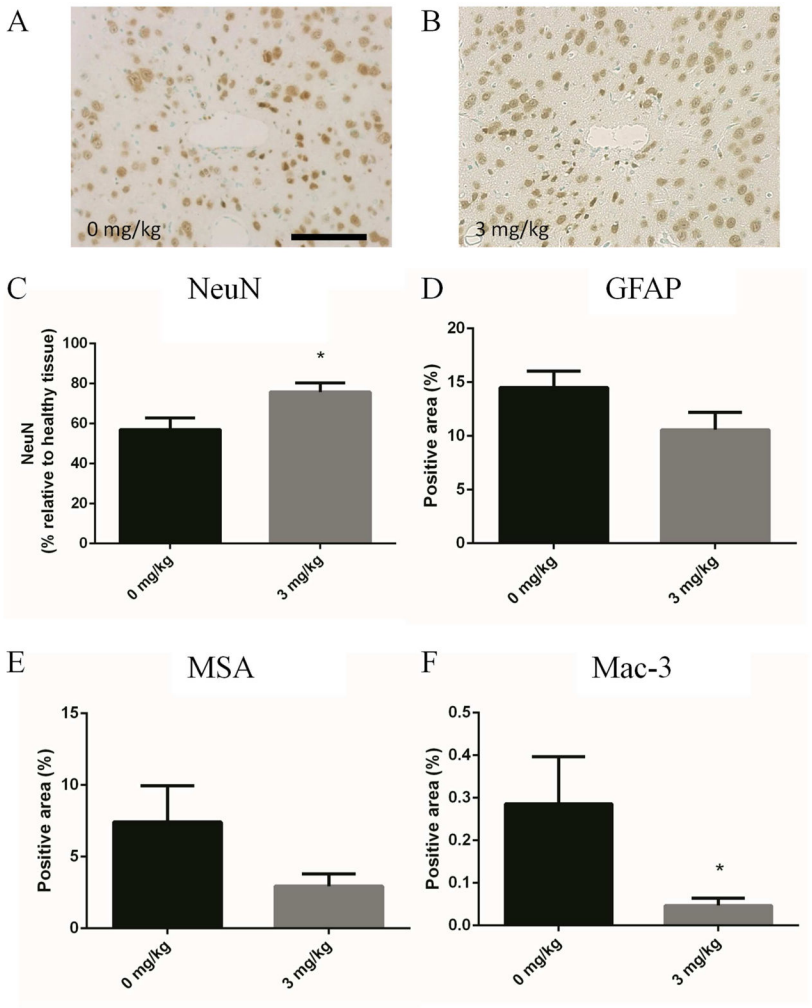

Figure 4.

Delivery of the CCR2 agonist RS 102895 reduces neuroinflammation at 2 wks. Implant bearing mice were given IP injections of RS 102895 every day for 2 wks at doses of 3.0 and 0 mg/kg. Immunohistochemical stain for NeuN (A, B, C) showed an increased neuronal density in the KO mice (B) when compared to the WT mice (A) with treatment, which agrees with the KO mouse phenotype. IHC stains for GFAP (D), MSA (E), and Mac-3 (F) all showed reduced neuroinflammation with RS 102895 treatment. * indicates $p < 0.05$ using Student's t test, n is 6 for each point and data is presented ± SEM.

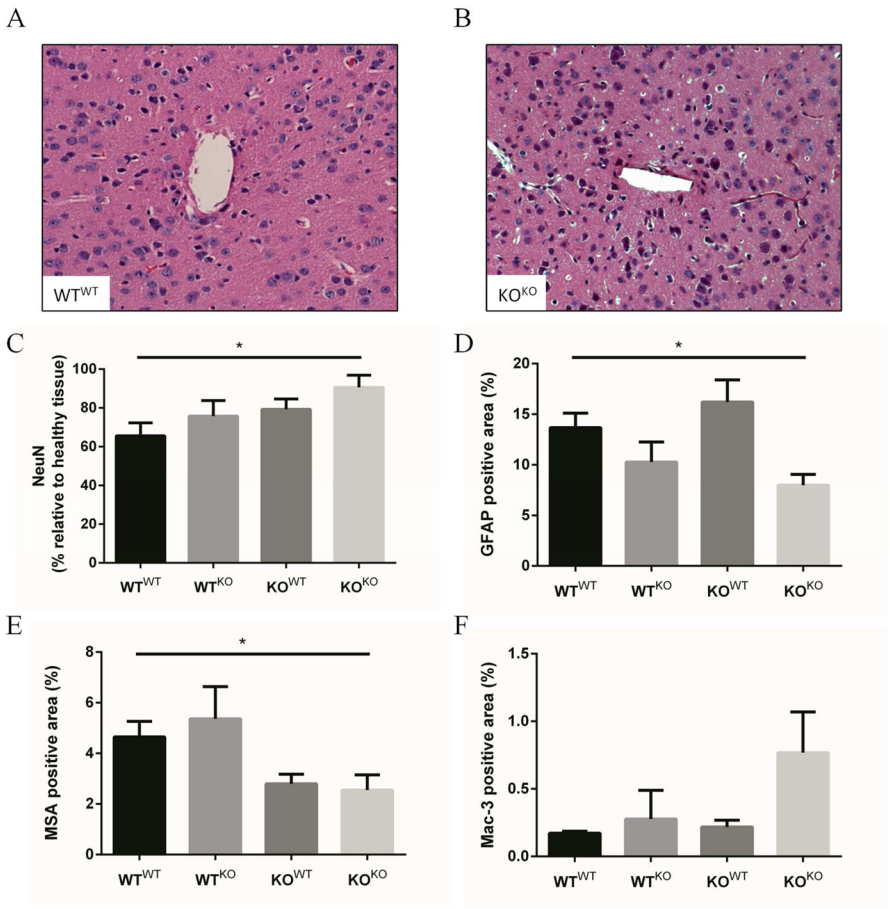

Figure 5.

Bone marrow chimeras indicate that reduction of MCP-1 signaling reduces neuronal loss. Lethally irradiated BL6 and MCP-1 KO mice were rescued with bone marrow from either KO or BL6 mice, resulting in WT^{WT}, WT^{KO}, KO^{WT}, and KO^{KO} mice (where the capital letter indicates the background of the recipient and the superscript letter indicates the genotype of the donor). WT^{WT} (A) and KO^{KO} (B) mice maintained neuronal densities similar to their background strain; however, WT^{KO} and KO^{WT} mice showed an intermediate response to decreased or introduced MCP-1 exposure, respectively (C). The amount of reactive astrocytes and inflammatory cells were similar to values observed during phenotypic characterization (D and F). BBB leakage appeared to decrease in both KO^{WT} and KO^{KO} mice, showing a host dominated response (E). * indicates $p < 0.05$ using Student's t test, n is 4 for WT^{WT}, WT^{KO}, and KO^{WT} and 6 for KO^{KO}, data is presented ± SEM.